

Explosive Nucleosynthesis in Astrophysics^{*}

CHEN Yong-Shou^{1,2} SHU Neng-Chuan¹ WU Kai-Su¹

¹(China Institute of Atomic Energy, Beijing 102413, China)

²(Institute of Theoretical Physics, CAS, Beijing 100080, China)

Abstract The nuclear processes in astrophysics are briefly reviewed, and the explosive hydrogen burning are addressed and calculated with some new reaction rates obtained from the most recent experimental data. We pointed out that the reaction flux from the hot pp-chain into the CNO cycle through the proton capture on ^{11}C may overcome the flux through the 3α process. The abundance of ^{18}F calculated with the new rates of the $^{18}\text{F}(p, \gamma)$ and (p, α) is 1.8 times larger than the previous one. The calculated results of the rp-process at the typical condition of the X-ray burst show that the abundances of the waiting point nuclei ^{89}Ru and ^{93}Pd , using the recent experimental β -decay life times, are about 4 times larger than the previous ones.

Key words nucleosynthesis, rp-process, capture reaction

1 Introduction

The nuclear processes in astrophysics can be derived assumably into two categories according to their processing timescales, the explosive and hydrostatic nuclear burnings. The nuclear reaction process in the stellar evolution is a typical hydrostatic nuclear burning, while the nucleosynthesis process in a supernovae event is an explosive nuclear burning. The reaction paths of the different nuclear processes are different in going through the regions of nuclei. The reaction path is defined by the general reaction flow for the each type of nuclear processes, and can be presented in the nuclear chart. The stellar evolution nuclear process synthesizes elements up to the iron region and its path is closely along the β -stability line. The slow neutron capture (s-)process has the nature of non-explosive events and passes also along the valley of the stability, but producing heavier nuclei up to the Pb region. The fast neutron capture (r-)process is an explosive one, expected to occur in supernovae, for example, and has its path going through the very neutron rich region, producing very heavy nuclei up to the actinides. The rapid proton capture (rp-)process is also explosive one, occurring in the X-ray bursts, for example, and has its path near the proton drip

line, producing nuclides beyond mass 80 region, however, the end point of the rp-process is still a problem open to answer. We shall address on the rp-process in the present study by using some new rates of the proton capture reactions obtained from the recent measurements. The impacts of these new rates on the underline nuclear burning processes will be discussed in some details.

The scenarios of the rp-process are discussed in Section 2. Section 3 is a brief description of the reaction network equation and the reaction rate. The calculated results of the networks for the hot p-p chain, the CNO cycle and the rp-process are shown in Section 4. Few remarks are given in Section 5.

2 Scenarios of the rp-process

The scenarios of astrophysical nucleosynthesis are important subjects in the study of nuclear astrophysics. The relatively well known scenarios are those for the hydrostatic stellar nuclear burning and for the s-process, which are all non-explosive. The s-process nucleosynthesis has been identified to occur in the Asymptotic Giant Branching (AGB) stars, with masses of 1—5 sun mass, which is driven mainly by the

Received 29 November 2003, Revised 29 March 2004

^{*} Supported by National Natural Science Foundation of China(19935030, 10075078, 10047001) and Major State Research Development Program of China (G20000774)

neutron source reaction $^{13}\text{C}(\alpha, n)^{16}\text{O}$. The scenarios of the explosive nucleosynthesis, such as for the rp-process and the r-process, are not well known and have often caused big debates. Particularly, the r-process sites are much less known, but the most probable sites are in supernovae. The scenarios for the rp-process are relatively well known to be associated with the accreting binary star systems, such as nova, the X-ray bursts, Type Ia supernova and the black hole disks. All these binary systems have a common structural character, namely involving the compact object star accreting the hydrogen rich material from the company giant star. Low accreting rate will lead to the pileup of fresh hydrogen and the ignition of hydrogen burning via the hot pp-chain reactions in an environment supported by the electron degeneracy pressure. Once the critical mass is reached in the layer the great enhancements of the rates of the reactions are obtained. On white dwarfs, as the compact object star, this triggers the novae events, and on neutron stars it leads to the X-ray bursts. High accretion rate gives rise to a high temperature but less degeneracy conditions in the envelope, and usually the stable hydrogen burning or weak flash. High accreting rates on white dwarfs may cause the Type Ia supernovae, while high accreting rates on neutron stars may result in the X-ray pulsars. The black hole accretion disks are expected also to be the sites of the rp-process in the conditions of relatively low density and high temperature. On a very low mass black hole of 10^4 sun mass has a typical density and temperature for the disk burning, $\rho = 10^3\text{--}10^5\text{g/cm}^3$ and $T_9 = 1.5$, where $T_9 = 1$ denote $T = 10^9\text{K}$, and the typical timescale of processing is $10^4\text{--}10^5$ seconds. The typical temperature and density for novae is $T_9 = 0.4$ and $\rho = 10^3\text{--}10^4\text{g/cm}^3$, and its timescale is $100\text{--}1000$ seconds. For the X-ray bursts the typical temperature and density is $T_9 = 1.5$ and $\rho = 10^6\text{g/cm}^3$, and the timescale is $10\text{--}100$ seconds.

3 The network equation and reaction rates

The nuclear reaction network equation describes the time evolution of isotope abundances, the amount of energy released by nuclear reactions and the reaction path and so on, in the nuclear process at some certain astrophysical conditions. The reaction network is mathematically a set of the non-linear differential equations which describe the time evolution of the isotope abundances $Y_i = X_i/A_i$, mass fraction divided by mass number, and may be written as

$$\frac{dY_i}{dt} = \sum_j N_j^i \lambda_j Y_j + \sum_{j,k} N_{j,k}^i \rho N_A \langle \sigma v \rangle_{jk,i} Y_j Y_k + \sum_{j,k,l} N_{j,k,l}^i \rho^2 N_A^2 \langle \sigma v \rangle_{jkl,i} Y_j Y_k Y_l. \quad (1)$$

Where $Y_i = n_i/\rho N_A$ is the abundance of species “ i ”, N_A is Avogadro constant number, n_i is the number density and ρ denotes the density. The first term in the equation includes the β -decays and photodisintegrations of all nuclei “ j ” producing nucleus “ i ” or destroying nucleus “ i ” if $j = i$, where λ_j is the decay constant. The second term describes the two particle reactions between nuclei “ j ” and “ k ”, producing or destroying nucleus “ i ”, where the $\langle \sigma v \rangle_{jk,i}$ stands for the thermonuclear reaction rates as defined by Fowler et al. in Ref. [1]. The third term describes the reactions between three particles “ j ”, “ k ” and “ l ”, forming or destroying nucleus “ i ”. The coefficients N_j^i , $N_{j,k}^i$ and $N_{j,k,l}^i$ describe how many particles of species “ i ” are produced ($N > 0$ if $i \neq j, k$ or l) and destroyed ($N < 0$ if $i = j, k$ or l) in the reaction and include the statistical factors for avoiding double counting the reactions among the identical particles. For example, $N_{j,k,l}^i = 1/3$ for the reaction of $3\alpha \rightarrow ^{12}\text{C}$.

By assuming that the stellar gas is in the thermodynamic equilibrium, the velocities of the particles can be described by a Maxwell-Boltzmann distribution. The nuclear reaction rates in the stellar gas can be calculated from the cross sections by the expression,

$$\langle \sigma v \rangle = \sqrt{\frac{8}{\pi\mu}} (kT)^{-3/2} \int_0^\infty E \sigma(E) e^{-E/kT} dE. \quad (2)$$

Where μ is the reduced mass of the target-projectile system, the center of mass energy $E = \frac{1}{2} \mu v^2$, where v refers to the relative velocity between the interacting particles, and the k stands for the Boltzmann’s constant, and T denotes the temperature. The proton capture reactions are crucial for the rp-process and the cross section is related with the astrophysical S -factor by the expression,

$$\sigma(E) = \frac{S(E)}{E} e^{-2\pi\eta}. \quad (3)$$

Where the coulomb parameter, or Sommerfield parameter, $\eta = 2\pi Z_1 Z_2 e^2/hv$. Inserting Eq. (3) into Eq. (2), one obtains

$$\langle \sigma v \rangle = \sqrt{\frac{8}{\pi\mu}} (kT)^{-3/2} \int_0^\infty S(E) e^{-E/kT - b/\sqrt{E}} dE. \quad (4)$$

Where $b = 2\pi\eta \sqrt{E}$, and thus the exponential term in the integral has a peak shape as a function of E , which is called as the Gamow-window. For the rp-process, the Q -values for the proton capture (p, γ) reactions drop down rapidly near

the proton drip line and, therefore, the compound nuclei are often formed in the low excitation energies. The reaction rates are then dominated often by only one or two resonance levels located in the Gamow-window, in other words, the rp-process requires detailed nuclear structure inputs. The astrophysical S -factor is more frequently employed rather than the cross section in the astrophysics studies since the former is usually a quite flat function of the center of mass energy so that the extrapolations to the zero energy will have much less uncertainties.

4 The calculated results and discussions

The reaction rates can be calculated from the cross section or the S -factor by using the expression as given in the previous section. In the presence of hydrogen, the nuclear burning proceeds via the rapid proton capture reactions (rp-process)^[2]. The rp-process contains a sequence of proton capture and β -decays, and is responsible for the burning of hydrogen into heavier elements. The rates for proton captures are the key-important inputs for the rp-process network calculations. Unfortunately, the required capture rates for the rp-processes are poorly known experimentally since the related nuclei are unstable. The radiative beams provide opportunities to access the proton rich region, however, the extrapolation or interpolation are often needed to obtain the cross sections or S -factors at the stellar energies. The most of the rates have to be calculated by the various theoretical models, while the key-important reactions should be measured experimentally.

4.1 $^{18}\text{F}(p, \gamma)^{19}\text{Ne}$ and $^{18}\text{F}(p, \alpha)^{17}\text{O}$ reactions

Recently, we have obtained the new rates for the $^{18}\text{F}(p, \gamma)^{19}\text{Ne}$ and $^{18}\text{F}(p, \alpha)^{17}\text{O}$ reactions, in collaboration with ORNL^[3]. There are 30 resonances in the compound nucleus ^{19}Ne , being identified to contribute to the reaction rates as they are located within the Gamow-window. The 20 of them are known experimentally for the resonance parameters, and the 10 rests are unknown missing levels. The properties of these missing resonance levels and their contributions to the rates were calculated theoretically and added to the total rates, and the resonance parameters of the 20 known level were examined and upgraded. The obtained new rates are different from the previous rates obtained by Coc et al. (2000)^[4]. The importance of the $^{18}\text{F}(p, \gamma)$ and (p, α) reac-

tions can be found in the fact that the CNO cycle may break out into the rp-process if the rate of the (p, γ) reaction sufficiently larger than that for the (p, α) reaction, which leads back to the CNO cycle. The network calculation are carried out by using these new rates at the typical conditions of a nova explosion in an "ONeMg" white dwarf star (peak temperature $T_9 = 0.4$ and density $\rho = 5 \times 10^4 \text{g/cm}^3$). The calculated CNO abundances as functions of the processing time are shown in Fig. 1. It is seen from Fig. 1 that the dramatic

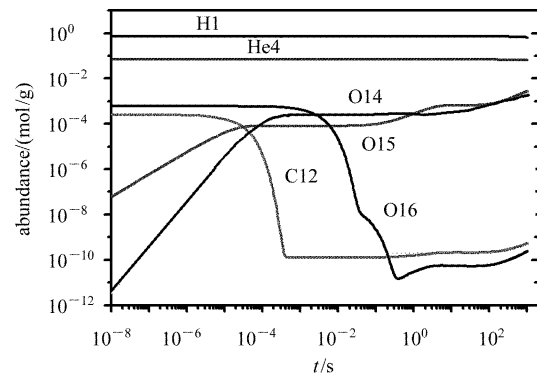


Fig. 1. The calculated CNO abundances as functions of the processing time at $T_9 = 0.35$ and $\rho = 5 \times 10^4 \text{g/cm}^3$, as the typical conditions for an "ONeMg" white dwarf nova.

increase in the abundances of both ^{14}O and ^{15}O before $t = 10^{-3} \text{s}$ is mainly caused by the converting initial ^{12}C into these two nuclei through the explosive hydrogen burning of the CNO cycle. While the further risings in the ^{15}O and ^{14}O abundances after few and ten seconds, respectively, are contributed from the converting ^{16}O . After about hundred seconds the ^4He is converted into ^{12}C and ^{16}O . The relatively flat curves of all the isotopes after few seconds indicate that the CNO cycle reaches its approximate steady state. The calculated results show that the synthesized abundance of ^{18}F , not plotted in the Figure, is 1.8 times of that given in the calculation of Coc et al.^[4]. The radioactive decay of the long-lived isotope ^{18}F is the strongest observable γ -ray source in novae^[5]. The γ ray emission in novae during the first several hours after the explosion predominantly at energies of 511keV and below is produced by electron-positron annihilation in the expanding envelope and the subsequent Compton scattering of the resulting γ -ray photons. The ^{18}F is most important positron source because of the relatively large its abundance, and because the relatively long half-life of ^{18}F , $\tau = 109.8 \text{m}$, enable positrons to be emitted after the expanding envelope becomes transpar-

ent to γ -ray radiation^[5]. The more abundance of ^{18}F implies the higher intensity of the γ -ray can be expected to benefit the observations. For the typical X-ray burst conditions (temperature $T_9 = 1.5$ and density $\rho = 1.5 \times 10^6 \text{ g/cm}^3$) the rp-process network calculation was carried out, and the results indicate that the transition from the CNO cycle to the rp-process hydrogen burning at higher mass nuclei mainly occurs via $^{18}\text{Ne}(\alpha, p)^{21}\text{Na}$ rather than $^{18}\text{F}(p, \gamma)^{19}\text{Ne}$ or $^{15}\text{O}(\alpha, \gamma)^{19}\text{Ne}$.

4.2 $^{11}\text{C}(p, \gamma)^{12}\text{N}$ reaction

The $^{11}\text{C}(p, \gamma)^{12}\text{N}$ cross section is calculated by assuming that the reaction proceeds by direct E1 capture of protons to the ground state of ^{12}N , and that the initial and final states of the system can each be described by a single particle model of a proton moving in an optical potential that represents its interaction with the ^{11}C ground state. The capture cross section for emission of electric dipole radiation can be calculated by the expression

$$\sigma_1 = \frac{16\pi}{9} \left(\frac{E_\gamma}{\hbar c} \right)^3 \frac{1}{\hbar v} \frac{1}{(2I_1 + 1)(2I_2 + 1)} \sum_m \sum_{I_m} |T_{1m}|^2. \quad (5)$$

Where E_γ is the γ -ray energy, v is the relative velocity between particles 1 and 2, I_i is the spin of particle i , and I stands for the channel spins of initial and final states, anticipating that they will be the same. The E1 transition matrix element T_{1m} may be written as,

$$T_{1m} = \langle I_{p,^{11}\text{C}}^{12}\text{N}(\mathbf{r}) | e_{\text{eff}} r Y_{1m}(\Omega) | \psi_k^{(+)}(\mathbf{r}) \rangle, \quad (6)$$

where the effective charge $e_{\text{eff}} = eN/A$ for proton capture reaction, N and A is the neutron and mass numbers of the whole system respectively. The overlap function of the bound state wave functions of ^{12}N , ^{11}C and p (proton) is expressed by

$$I_{p,^{11}\text{C}}^{12}\text{N}(\mathbf{r}) = \langle \phi_p(\xi_p) \phi_{^{11}\text{C}}(\xi_{^{11}\text{C}}) | \phi_{^{12}\text{N}}(\xi_p, \xi_{^{11}\text{C}}, \mathbf{r}) \rangle, \quad (7)$$

where \mathbf{r} is the distance vector between the centers of mass of proton and ^{11}C and ξ_s are the intrinsic coordinates for the particles indicated by their footmarks. The radial part of the overlap function, $I_{l_j, I}(r)$, depends on the relative orbit angular momentum l_j of the captured proton and the ^{11}C core in the bound state j_f of ^{12}N and the channel spin I . At very low energies of astrophysical interest, the capture reaction is almost totally peripheral and thus the radial overlap function has the asymptotic behavior,

$$I_{l_j, I}(r) = C_{l_j, I} W_{\eta, l_j + 1/2}(2\kappa r) / r (r \geq R_N). \quad (8)$$

Where $C_{l_j, I}$ is the Asymptotic Normalization Coefficient

ANC, the amplitude of the tail of the radial overlap integral. $W_{\eta, l_j + 1/2}(2\kappa r)$ is the known Whittaker function, the wave number for the bound state $\kappa = \sqrt{2\mu E_B} / \hbar$, here μ is the reduced mass, E_B is the binding energy. $\psi_k^{(+)}(\mathbf{r})$ is the entrance channel distorted wave function, describing the relative motion between ^{11}C and proton in the continuum, can be calculated by DWBA. R_N is the nuclear interaction radius between proton and ^{11}C . Therefore, it is the ANC value that determines the capture cross section and thus the normalization of the astrophysical S -factor.

The angular distribution of the $^{11}\text{C}(d, n)^{12}\text{N}$ reaction at $E_{c.m.} = 9.8 \text{ MeV}$ was measured in inverse kinematics with the secondary ^{11}C beam^[6]. By carrying out the DWBA analysis, the asymptotic normalization coefficient (ANC) for the virtual decay $^{12}\text{N} \rightarrow ^{11}\text{C} + p$ was extracted to be $2.86 \pm 0.91 \text{ fm}^{-1}$. The zero energy astrophysical S -factor for the direct capture of $^{11}\text{C}(p, \gamma)^{12}\text{N}$ reaction was obtained as $S(0) = 0.157 \pm 0.050 \text{ keV b}$, by carrying out the radioactive capture calculation with the derived experimental ANC and the above expressions of Eqs. (3, 5—8). The two lowest resonances in ^{12}N , namely 2^+ ($E_{c.m.} = 0.360 \text{ MeV}$) and 2^- ($E_{c.m.} = 0.591 \text{ MeV}$), were examined and their contributions to the reaction rates were calculated and compared with the calculated direct capture rate in Fig.2. It can be seen that the direct capture dominates the total reaction rate of $^{11}\text{C}(p, \gamma)^{12}\text{N}$ in the wide energy range of astrophysical interest, and this result is different from what expected in previous work where the resonance 2^- was speculated to dominate^[7].

With the new reaction rates we have carried out calculation of the network for the hydrogen burning from the hot pp-

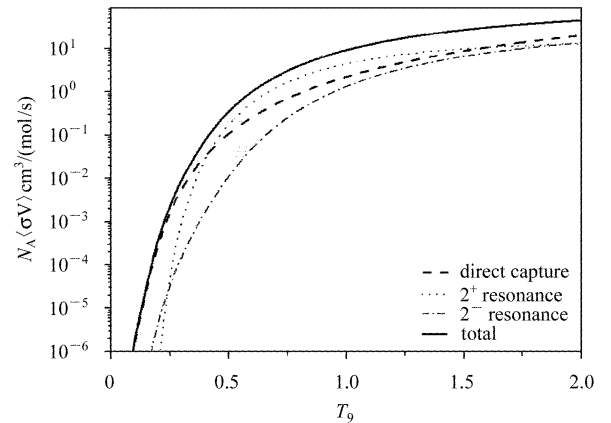


Fig.2. The reaction rates of $^{11}\text{C}(p, \gamma)^{12}\text{N}$ reaction as a function of temperature. Note that the direct capture dominates the total rate at the stellar temperatures, $T_9 < 0.4$.

chain to the CNO cycle in the astrophysical environment of a very metal-poor massive star. For the typical conditions of temperature $T_9 = 0.25$ and density $\rho = 10^3 \text{ g/cm}^3$, the calculated abundances and the reaction flux from the pp-chain into the CNO cycle are plotted as functions of the processing time in Fig.3. It is seen in Fig.3 that the abundance of ^3He drops

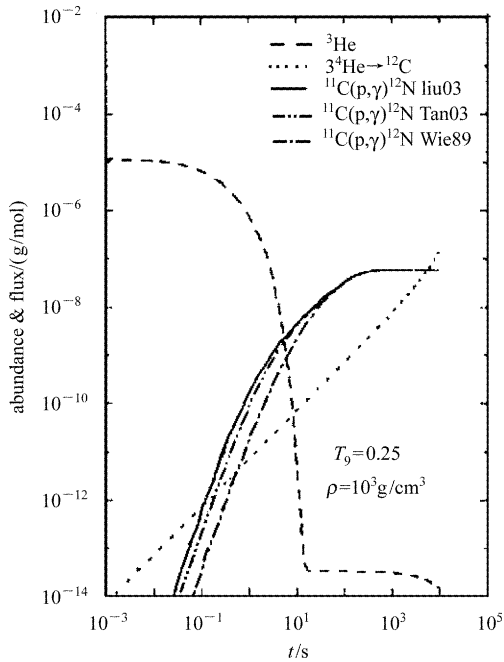


Fig.3. The calculated abundances and the reaction flux from the pp-chain into the CNO cycle as functions of the processing time at the typical astrophysical conditions for a very metal-poor massive star, $T_9 = 0.25$ and $\rho = 10^3 \text{ g/cm}^3$. The initial abundances used are the solar abundances. Note that the flux for $^3\text{He}(\alpha, \gamma)^7\text{Be}(\alpha, \gamma)^{11}\text{C}(\text{p}, \gamma)^{12}\text{N}$ can overcome that for the triple-alpha process.

very quickly and is almost exhausted at 10^4 s , this is responsible for the fast rising of the flux into the CNO cycle through the reaction chain $^3\text{He}(\alpha, \gamma)^7\text{Be}(\alpha, \gamma)^{11}\text{C}(\text{p}, \gamma)^{12}\text{N}$, converting ^3He into the CNO material. The striking feature is that the burning process via this reaction chain starting from ^3He into the CNO may overcome the process of the triple-alpha producing ^{12}C as long as the pre-existing ^3He is burned off, and this is also true if one uses the other two different rates obtained from the different direct capture S -factors taken in Refs. [8] and [9], as shown in Fig.3. The very metal poor massive and supermassive stars of the first generation after the big bang will have no CNO, this would enable them to undergo the typical CNO cycle hydrogen burning. The well known way to produce the CNO nuclei during stellar evolution is via

the triple-alpha reaction producing ^{12}C . An alternative way, as suggested in the present calculation, is to convert the pre-existed ^3He into the CNO material via the above reaction chain where the most important reaction link is $^{11}\text{C}(\text{p}, \gamma)^{12}\text{N}$. The energy generation in the stellar evolution is mainly during the stage of the hydrogen burning in the CNO cycle. The sufficiently large rate of the above reaction chain starting from ^3He will speed the bridging process from the hot pp-chain into the CNO cycle and therefore affect the stellar evolution. The present calculation reveals the importance of the link reaction $^{11}\text{C}(\text{p}, \gamma)^{12}\text{N}$, however, the uncertainties of its cross section at stellar energies are still quite large. Moreover, the direct proton capture on ^{11}C has been measured indirectly by means of the ANC method and yielded different values of S -factors. It would be worth to perform the direct measurements of $^{11}\text{C}(\text{p}, \gamma)^{12}\text{N}$ reaction to reduce the uncertainties in the reaction rates for both the direct and resonance captures. This coming work have been recently approved with the title of "Direct Measurement of Astrophysical $^{11}\text{C}(\text{p}, \gamma)^{12}\text{N}$ Reaction at GRAGON", as the TRIUMF experiment, and will be performed by the international collaboration headed by Liu, CIAE.

4.3 The rp-process in the X-ray bursts

In the X-ray binary systems a neutron star accretes hydrogen and helium rich matter from the envelope of a close companion giant star. The accreted material is compressed, heated, and eventually undergoes thermonuclear burning, the rp-process. The end point of the rp-process has not well understood. Many early rp-process calculations for the X-ray bursts were performed with the reaction networks that ended at ^{56}Ni . For these calculations the reason was argued that further proton captures were negligible for the small rates caused by the increasing Coulomb barriers. The later calculations were simulations with larger networks up to the Kr region^[10]. Recently a parameter study was performed with an updated and extended network up to the Sn region^[11]. The intention of the present study is to evaluate the nuclear reaction sequences for conditions in explosive hydrogen burning and to investigate the influence of improved reaction rates and new experimental β -decay rates for the nucleosynthesis in hot hydrogen burning at the X-ray burst conditions. To analyze this influence in a clear fashion we perform our calculations with constant temperature and density. The time integrated rp-process reaction flow during the X-ray burst was calculated at the typical con-

ditions of temperature $T_9 = 1.5$ and density $\rho = 1.5 \times 10^6 \text{g/cm}^3$. The capture reaction rates, the photodisintegration rates and the β -decay lifetimes are the main nuclear inputs for the rp-process network calculations. For the present study we employed two sets of the nuclear input data: the standard one, denoted by "Schatz98", which is as the same as Schatz et al. 's^[11] and the present set, denoted by "Xu03", in which the new experimental β -decay lifetimes for five nuclei ^{93}Pd , ^{92}Rh , ^{89}Ru , ^{85}Mo and ^{81}Zr were used to replace the theoretical β -decay lifetimes for these five nuclei in the standard data set. The experimental β -decay lifetimes for the above five nuclei were taken from Ref. [12].

The nuclear reaction network includes all proton rich nuclei from hydrogen to isotopes over the $A = 100$ region. Helium burns via mainly the triple-alpha reaction and the α -process, a sequence of alternating (α, p) and (p, γ) reactions into the $A = 60$ region. The seed nuclei for the rp-process are provided by these helium burning processes. The calculated time integrated reaction flow over 30 seconds for the rp-process starting from the $A = 70$ to $A = 100$ regions are

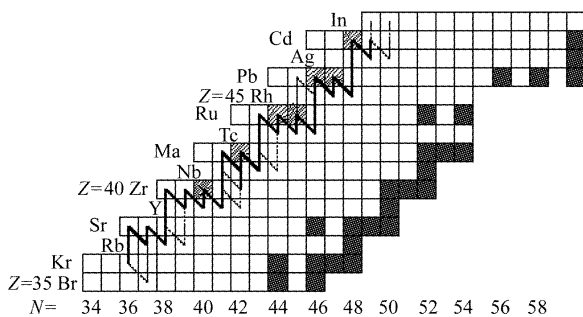


Fig.4. The calculated reaction flow integrated over 30s for the rp-process at the typical conditions of temperature $T_9 = 1.5$ and density $\rho = 1.5 \times 10^6 \text{g/cm}^3$ for the X-ray bursts. The heavy solid lines showing the main path of the rp-process denote a flux of $10^{-2}(\text{mol/g})$, and the dash lines stand for a flux of $10^{-3}(\text{mol/g})$. The waiting point nuclei are shown in shade, and the stable nuclei in black.

shown in Fig.4. The heavy solid lines showing the main path of the rp-process denote a flux of $10^{-2}(\text{mol/g})$, and the dash lines stand for a flux of $10^{-3}(\text{mol/g})$. Along the reaction path of the rp-process there exist some waiting point nuclei which play an particularly important role in controlling the process. At a waiting point nucleus, the Q -value of (p, γ) reaction is small or negative, so that the photodisintegration could restrain the occurrence of the (p, γ) reaction, and the

nucleus has to wait for the β -decay to continue the process. The waiting point nuclei will store the produced material until the burning is over. Therefore, the long lived waiting point nuclei along the reaction path will store some more material at the end of the rp-process. The detailed analysis of the calculated reaction flux patterns suggests some waiting point nuclei in the $A = 80-100$ region, ^{80}Zr , ^{84}Mo , $^{88,89}\text{Ru}$, $^{92,93}\text{Pd}$ and ^{96}Cd . The experimental β -decay lifetimes for ^{93}Pd , ^{92}Rh , ^{89}Ru , ^{85}Mo are $\tau_{1/2} = 1.3, 3.0, 1.2, 3.2\text{s}$ respectively, which are all about ten times larger than the theoretical values of $\tau_{1/2} = 0.224, 0.347, 0.294, 0.368\text{s}$, respectively, taken from Ref. [11]. Therefore, the more abundances of these nuclei are expected if the experimental half-life data are used. Among the above waiting point nuclei, the β -delayed proton decay of ^{89}Ru and ^{93}Pd have been measured. As an example, the abundances of the waiting point nucleus ^{93}Pd as functions of the processing time, calculated with both theoretical and experimental β -decay lifetimes, are shown in Fig.5.

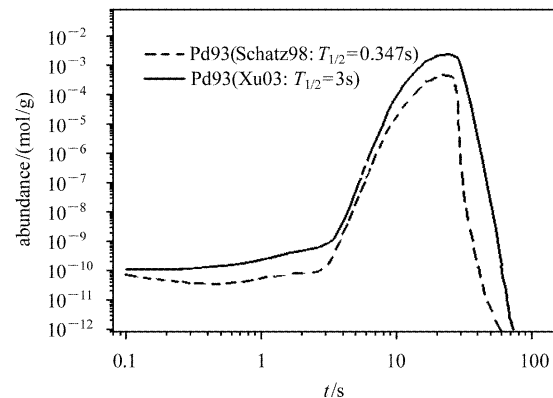


Fig.5. Calculated abundance of ^{93}Pd as a function of the processing time for the rp-process at the typical conditions of the X-ray bursts as the same as in Fig.4. Note that the experimental β -decay lifetime leads to a higher abundance (solid line) than one given by the theoretical life time (dash line).

It can be seen that the calculated abundance of ^{93}Pd with the experimental lifetime is about 4 or more times larger than that with the theoretical lifetime during the entire processing time.

5 Summary

In summary, the new rates of $^{18}\text{F}(p, \gamma)$ and (p, α) were obtained, and the network calculation with new rates shows that in the X-ray burst burning the break out of the HCNO cycle mainly occurs via $^{18}\text{Ne}(\alpha, p)^{21}\text{Na}$ rather than $^{18}\text{F}(p, \gamma)^{19}\text{Ne}$ or $^{15}\text{O}(\alpha, \gamma)^{19}\text{Ne}$. But the new rates lead to a 1.8 times

higher abundance of ^{18}F in the typical Novae conditions. This is expected to benefit the observations of the novae events since the strongest observable γ -ray source in novae is believed to be associated with the positron decay of the long-lived isotope ^{18}F . The new rates of $^{11}\text{C}(p, \gamma)^{12}\text{N}$ were obtained, and the network calculations at the typical conditions for the very metal poor massive stars show a striking feature that the flux into the CNO cycle through the reaction chain $^3\text{He}(\alpha, \gamma)^7\text{Be}(\alpha, \gamma)^{11}\text{C}(p, \gamma)^{12}\text{N}$ may overcome the process of the triple-alpha producing ^{12}C as long as the pre-existing ^3He is burned off. The calculation of reaction flow shows that the rp-process at the X-ray burst conditions may proceed to

the $A = 100$ region during the timescale of the explosion. The calculated flux patterns suggest the waiting point nuclei in the $A = 80-100$ region, ^{80}Zr , ^{84}Mo , $^{88,89}\text{Ru}$, $^{92,93}\text{Pd}$ and ^{96}Cd . Among them, the experimental β -decay lifetimes were measured recently for ^{93}Pd and ^{89}Ru , which lead to about 4 times more abundances for these two nuclei than that given by the theoretical lifetimes. The network description of the nucleosynthesis in astrophysics requires completed and detailed nuclear structure and reaction informations, particularly for unstable nuclei. The radiative capture reaction rates and β -decay constants are crucial for the description of explosive nucleosynthesis.

References

- 1 Fowler W A, Caughlan G R, Zimmerman B A. *AR & A*, 1967, **5**: 525
- 2 Wallace R K, Woosley S E. *Astrophys. J. Suppl.*, 1981, **45**: 389
- 3 Shu N C et al. *Chin. Phys. Lett.*, 2003, **20**: 1470
- 4 Coe A et al. *Astron. Astrophys.*, 2000, **357**: 561
- 5 Hernanz M et al. *Astrophys. J.*, **526**: L97
- 6 LIU W P et al. *Nucl. Phys. A*, 2003, **728**: 275
- 7 Descouvemont P. *Nucl. Phys. A*, 1999, **646**: 261
- 8 TANG X et al. *Phys. Rev. C*, 2003, **67**: 015804
- 9 Timofeyuk N K et al. *Nucl. Phys. A*, 2003, **713**: 217
- 10 Fujimoto M Y, Sztajino M et al. *Astrophys. J.*, 1987, **319**: 902
- 11 Schatz H et al. *Phys. Rep.*, 1998, **294**: 167
- 12 LI Z K et al. *Eur. Phys. A*, 1999, **5**: 351; XU S W et al. private communication, 2003, IMPL, China

天体物理中爆发性核合成*

陈永寿^{1,2} 舒能川¹ 吴开谔¹

1(中国原子能科学研究院 北京 102413)

2(中国科学院理论物理研究所 北京 100080)

摘要 简要地评述天体核过程,着重讨论爆发性氢燃烧过程,并利用最新的反应率实验数据对氢燃烧过程进行了计算.指出从热 pp 链通过 ^{11}C 的质子辐射俘获反应进入 CNO 循环的反应流量可以超过 3α 过程的流量.用 $^{18}\text{F}(p, \gamma)$ 和 (p, α) 反应的新反应率计算的 ^{18}F 生成丰度比旧反应率给出的丰度要大 1.8 倍.对在 X 射线爆的典型天体物理条件下的快质子(rp)过程的计算表明,“等待核” ^{89}Ru 和 ^{93}Pd 的 β 衰变寿命的新实验数据给出的该 2 核的生成丰度,比旧实验数据给出的值要大 4 倍.

关键词 核合成 快质子(rp)过程 俘获反应